Available online at www.sciencedirect.com

ScienceDirect

Procedia Computer Science 256 (2025) 731–738

Procedia Computer Science

www.elsevier.com/locate/procedia

CENTERIS - International Conference on ENTERprise Information Systems / ProjMAN - International Conference on Project MANagement / HCist - International Conference on Health and Social Care Information Systems and Technologies

K-operator as a predictor for Alzheimer-Perusini's disease

Maria Mannone[a,b,c,*], Norbert Marwan[b,d,e], Peppino Fazio[c,f], Patrizia Ribino[a]

[a]*Institute for High-Performance Computing and Networking (ICAR), National Research Council (CNR), Italy*
[b]*Institute of Physics and Astronomy, Universität Potsdam – Germany*
[c]*Dipartimento di Scienze Molecolari e Nanosistemi (DSMN), Università Ca 'Foscari di Venezia – Italy*
[d]*Potsdam Institute for Climate Impact Research (PIK), Member of the Leibniz Association – Germany*
[e]*Institute of Geosciences Potsdam, University of Potsdam – Germany*
[f]*VSB, Technical University of Ostrava– Czechia*

Abstract

Progressive memory loss occurring in age-related neurological diseases contributes to the disgregation of the individual, with serious personal and social consequences. We model the brain network damage provoked by a neurological disease through a physics-inspired mathematical operator, *K*. Acting on a diseased brain, *K* provides the disease time evolution. Focusing on Alzheimer-Perusini's disease (AD), we approximate the *K*-operator considering selected patients of the ADNI 2 dataset. We also propose *K* as a predictor for the disease progress over time and give its preliminary evaluation in the AD progression from the cognitive normal (CN) stage to AD through intermediate mild cognitive impairment (MCI) stages.

Keywords: : memory; Alzheimer; operator; matrix computation; ADNI

1. Introduction

Da che le mal vietate Alpi e l'alterna / Onnipotenza delle umane sorti

Armi e sostanze t'invadeano ed are / E patria e, tranne la memoria, tutto.

(From the undefended Alps and the alternate omnipotence of the human destinies,

[they] deprived you of weapons, country, richness, altars, and, beside memory, of everything).

Ugo Foscolo, Dei Sepolcri, vv. 182-185

Memory characterizes our identity, as individuals, countries, and species. The memory we carry with us wherever we go is stocked inside our neurons. However, neurological diseases can take it away. It is the case of the memory loss involved in Alzheimer's disease (AD), more properly denoted as Alzheimer-Perusini's disease after their discoverers, the German psychiatrist Alois Alzheimer (1864–1915) and the Italian physician Gaetano Perusini (1879–1915) [21, 3]. AD is a serious dementia characterized by a progressive loss of neurons and plaque alterations, causing cortical atrophy, whose symptoms also include progressive destruction of cognition in elderly adults [8]. As the world's population continues to grow older, there will be a rise in the number of people affected by AD. By

*Corresponding author
E-mail addresses: maria.mannone@icar.cnr.it

10.1016/j.procs.2025.02.173

2050, it is estimated that over 130 million elderly individuals worldwide will suffer from AD [23]. The AD progression can be conceptualized as a spectrum spanning from cognitively normal (CN) individuals through the early stages known as mild cognitive impairment (MCI), ultimately leading to AD. MCI individuals may be further categorized into two subgroups, specifically early MCI (EMCI) and late MCI (LMCI) [18].
AD currently lacks a definitive cure; however, available treatments have the potential to modulate the progression of the disease. Hence, it is imperative to devise novel approaches for identifying distinct AD stages to improve the comprehension of its pathophysiological progression, thereby facilitating preclinical studies of the disease.
Mainly, it is shown that higher AD damage is provoked in the brain's parietal and subcortical areas [3]. Some researches also indicate that these disorders are also linked to impaired neural connectivity throughout the entire brain [11, 10]. Adopting a computational approach to model brain connectivity can enhance understanding of changes in brain network architecture that may correspond to AD progression. Moreover, numerous neuroimaging methodologies are available for the visualization of both the structural and functional aspects of the human brain [25]. Among them, non-invasive resting-state functional magnetic resonance imaging (rs-fMRI) offers significant advantages in unravelling the intricate brain connectivity network, examining dynamic changes in brain function from EMCI to LMCI and AD [5] and elucidating fundamental aspects of the disease pathophysiology [13].
Recent years have seen a growing interest in utilizing graph-theoretical methods and complex network theory to model the brain as an interconnected network of brain regions [12, 1]. Hence, from the point of view of the brain network on AD, there is a decreasing trend of vertex strength and connectivity, and a shift toward a random-network architecture, jointly with a short-range link increase [11].
Following this trend, we adopt a new method inspired by theoretical physics, where the disease effect on the brain network is modelled as a mathematical operator, the *K*-operator (from *Krankheit*, German for *disease*) [22]. Such an operator is a mathematical object that models a neurological disease in terms of disruptions provoked on the brain network starting from rs-fMRI. In this study, we try to quantitatively compute the *K*-operator for AD, mainly focusing on modelling AD progression, using data provided by the Alzheimer's Disease Neuroimaging Initiative (ADNI).
Firstly, we have conducted an exploratory analysis of the ADNI dataset to collect statistical information about the characteristics of patients at different AD stages to obtain some preliminary indications that can guide our approach and validate it. Then, we applied the proposed mathematical model to selected ADNI patients by computing the related *K* operator and observing the disease's impact on temporal lobes, cingulate cortex, and subcortical brain structures, strictly related to memory effects. Hence, according to our findings, we sketch a prediction model of AD evolution given the rs fMRI of a patient at the baseline. Finally, we give a preliminary evaluation of the *K*-operator in the AD progression from the CN stage to AD through intermediate MCI stages.

2. Materials and Methods

Dataset. The present study relies on data gathered from ADNI, with a specific focus on the data derived from the ADNI 2 study. Such a study is a longitudinal investigation designed to identify and monitor clinical, imaging, genetic, and biochemical biomarkers for early AD detection. ADNI categorizes different AD stages for participants as healthy normal control (CN), Subjective Memory Complaints (SMCs), Mild Cognitive Impairment (MCI), and Alzheimer's Disease (AD) classes. In particular, ADNI 2 distinguished MCI into EMCI and LMCI. The progression from the EMCI stage to the LMCI is not reversible, which means that the patient's cognitive condition gets worse significantly.
In this paper, a subset of ADNI 2 data was used, including demographics, clinical, structural magnetic resonance imaging (MRI), and resting-state functional MRI (rs-fMRI). Mainly, demographics and clinical variables are considered to collect statistical information about the characteristics of patients at different AD stages and include Age, Sex, Education, Mini-Mental State Examination (MMSE), Clinical Dementia Rating (CDR-Global) and Clinical Dementia Rating Sum of Box (CDR-SB). CDR-Global and CDR-SB are measures that assess the severity of dementia based on six distinct domains reflecting various facets of cognitive compromise (i.e., memory, orientation, judgment and problem-solving, community affairs, home and hobbies, and personal care).
Regarding neuroimaging features, we considered MRI volumetric information to evaluate volume change in characteristic locations to different stages of AD disease that include the Ventricles, Hippocampus, Whole Brain, Entorhinal, Fusiform Gyrus, Middle Temporal Gyrus (MidTemp) and Intracerebral Volume (ICV). Conversely, we considered rs-fMRI connectivity analysis for identifying neurodegenerative diseases characterized by disruptions in brain network connectivity, before the onset of observable brain atrophy. The biomarkers based on both neuroimaging modalities are expected to have complementary information to improve the AD understanding.

Mainly, ADNI 2 collects data from 790 subjects at baseline. It contains individuals classified with subjective memory complaints that represent a concern of people with cognitive difficulties and are very common in elderly

individuals [15]. It is unclear whether SMCs are merely a normal age-related process [6]. Hence, for the scope of this study, we do not consider such kinds of patients. Moreover, we removed patients without completed records regarding all the features we considered in this study. Hence, 551 patients were identified for the exploratory analysis.

Statistical analysis on ADNI 2. At the baseline, 551 subjects were identified, including 186 (33.8%) CN individuals, 138 (25%) EMCI, 125 (22.7%) LMCI, and 102 (18.5%) AD patients. The findings of the statistical analysis performed on the ADNI 2 dataset, about demographics and clinical information, as well as brain volumetric data, are presented in the Appendix (see Tables 1 and 2). A p-value = 0.05 has been chosen to show statistical evidence.

Mainly, a Kruskal-Wallis H test was performed to evaluate statistical differences among CN, EMCI, LMCI and AD classes of patients for the Age variable that did not follow a normal distribution. A p-value = 0.0023 shows statistical evidence that a difference among groups exists. After a pairwise comparison with post-hoc Dunn's test, we can only assess that in ADNI 2, EMCI patients are younger than NC ($p = 0.02$) and AD ($p = 0.008$). Moreover, among all patients (i.e., 551), 52.8% are males, and 47.2% are females. We obtain that there is no different distribution for gender among groups ($p > 0.05$) as well as for education. A significant difference is highlighted among all four groups ($p \approx 0$) as concerns the MMSE score. The mean value of MMSE was 29.0±1.3 for CN, 28.4±1.6 for EMCI, 27.4±1.8 for LMCI and 23 ± 2.1 for AD individuals. In particular, the MMSE progressively decrease with the severity of the AD stage. Pairwise comparisons with post-hoc Dunn's test show that we may reject the null hypothesis ($p < 0.01$) for each pair of groups and conclude that the difference among the MMSE scores is statistically significant. Almost all cognitively normal subjects have no problem with memory, orientation, community&affairs, home&hobbies and personal care domains ($p \approx 0$). Only 3.8% of normal individuals show a slight impairment in the judgment and problem-solving domain. On the contrary, as the CDR-SB also highlights, almost all MCI and AD individuals show problems in the memory domain at different levels and other problems in different domains.

Finally, only the Intracranial Volume (ICV) does not show statistical difference among groups ($p = 0.34$), while significant differences are detected for all other variables and brain regions. In particular, the Entorhinal and Hippocampus show statistical differences among groups and correlation with AD. As known [14, 4, 26], the entorhinal-hippocampal system contains distinct networks subserving declarative memory. This system is selectively vulnerable to changes in ageing and pathological processes. The entorhinal cortex (EC) is a pivotal component of this memory system since it interfaces the neocortex and the hippocampus. The hippocampus and EC are brain areas most affected by Alzheimer's. In the early stages of AD, the hippocampus shows rapid loss of its tissue, which is associated with functional disconnection with other brain parts. In AD progression, atrophy of medial temporal and hippocampal regions are the structural markers in MRI. After executing a post-hoc Dunn's test for pairwise comparisons between groups, statistical evidence has been found that the hippocampus differs for each pair of groups ($pCN-EMCI = 4.8 \cdot 10-2$, $pCN-LMCI = 2.88 \cdot 10-9$, $pCN-AD = 1.8 \cdot 10-25$, $pEMCI-LMCI = 5.7 \cdot 10-5$, $pEMCI-AD = 2.6 \cdot 10-17$, $pLMCI-AD = 1.9 \cdot 10-5$) and decreases with AD progression. Conversely, there is no statistical difference between only CN and EMCI individuals in the Entorhinal Cortex, Fusiform Gyrus and Middle Temporal Gyrus ($pCN-EMCI = 0.37$, $pCN-EMCI = 0.76$, $pCN-EMCI = 0.86$, respectively). Statistical differences are shown in Ventricles only between CN, EMCI and LMCI with AD ($pCN-AD = 6.0 \cdot 10-8$, $pEMCI-AD = 9.6 \cdot 10-7$, $pLMCI-AD = 0.0023$). No statistical difference in Ventricles between CN and MCI.

K-operator and methodological approach. Following the notation in [22], we denoted the brain network as a blockmatrix G, where each diagonal block represents the connections between brain lobes, while the off-diagonal blocks indicate the inter-lobe connections. The K-operator acts upon the healthy brain G to generate a resulting state of the brain denoted as Gk, characterized by disease manifestations: $K\mathcal{G} = \mathcal{G}^k$ where the specific form of K depends upon the disease under study. Thus, considering as the starting point a brain already affected by the disease, K can model its progression as $K(t)\mathcal{G}^k$ (t)= $\mathcal{G}^k$ (t+1). Using as $\mathcal{G}^k$ (t), $\mathcal{G}^k$ (t+1) the connectivity matrices of the brain network of the same patient at two different time points, respectively, provided that $\mathcal{G}^k$(t) is invertible, we can obtain the K-operator as $K(t) = \mathcal{G}^k$(t+1)[$\mathcal{G}^k$ (t)]$^{-1}$.

Here, we adopt a hybrid technique, computing the elements of K using the element-wise product, obtaining the precise disease action on the corresponding pairs of ROIs; this yields symmetric and interpretable results, and the main patterns are qualitatively corresponding to the ones highlighted by the row-by-column product. Some comparisons are shown in section 3. Hence, we employ the following methodological steps to model the AD progression: (i) *Data preprocessing*: the raw rs fMRI data provided by ADNI are in DICOM format. Since the required format in most fMRI analysis tools is the NIfTI format, we convert the rs fMRI data from .dcm to .nii files; (ii) *Information retrieval*: brain-network and connectivity are obtained by processing .nii

files with Python library nilearn; (iii) *K-operator shape determination*: to compute the shapes of the K-operator experimentally in matrix form, we visualise the connectivity matrices for the brain networks, with the brain regions grouped into regions of interest (ROIs). The Multisubject dictionary learning [30] and the Harvard-Oxford [16] atlas are chosen as the brain atlas; (iv) *K-operator decomposition*: the decomposition of the K-operator according to its action on the specific brain lobes provides an agile tool to detect the presence and connectivity variations between brain areas. For the sake of simplicity, we will focus on the block-diagonal terms in this research. (v) *K-based prediction*: finally, given a patient baseline connectivity matrix, we can provide insights on the possible time evolution of the disease for the considered patient. In this article, we consider a simple linear regression.

3. Experimental Evaluation

For the experimental evaluation of k−operator, we chose seven patients with the following characteristics: Patient A (ID: 019 S 5019) is a 63-year-old AD female, with a middle-low education level (i.e., 12 years), an MMSE score of 21, showing problems in each CDR domain with a resulting CDR-SB = 6 and CDR = 1; Patient B (ID: 002 S 5018) is a 73-year-old AD male, with a middle-high education level (i.e., 17 years), an MMSE score of 23, showing minor problems than patient A in the domain of Community&Affair and Home&Hobby with a resulting CDR-SB = 5 and CDR = 1; Patient C (ID: 006 S 4153) is a 79-year-old AD male, with a high education level (i.e., 20 years), an MMSE of 22, with minor problems than patients A and B in all CDR domains with CDR-SB = 3 and CDR = 0.5; Patient D (ID: 018 S 4399) is a 78-year-old CN female, with a middle-high education level (i.e., 16 years), an MMSE of 28, without any problems in each of CDR domains with a resulting CDR-SB = 0 and CDR = 0; Patient E (ID: 012 S 4012) is a 71-year-old EMCI female, with a middle-high education level (i.e., 16 years), an MMSE of 28, initial problems in Memory, Orientation and Judgement, CDR-SB = 1.5 and CDR = 0.5; Patient F (ID: 031 S 4203) is a 77-year-old LMCI female, with a middle-high education level (i.e., 17 years), an MMSE of 26, showing higher problems in Memory, Orientation and Judgement than patient E and initial problem in Home&Hobby domain with a resulting CDR-SB = 4 and CDR = 0.5; Patient G (ID: 018 S 4696) is a 73-year-old AD female with a middle-high education level (i.e., 16 years), an MMSE of 16, showing higher problems in Memory, Orientation and Judgment than patient F and higher problems in Home&Hobby and personal care with a resulting CDR-SB = 9 and CDR = 1.

In particular, the last four patients have been selected to evaluate the evolution of the k-operator in the progression of Alzheimer's disease. Since we do not find patients with associate rs fMRI images that show all the stages of the AD progression, we try to select these patients according to statistical findings reported in Table 1 of the Appendix.

Evaluation of K-operators for AD patients. The analysis of Patient A* was made on her rs-fMRI at two different time points. The K-operator decomposed according to the brain macro-areas is shown as heatmaps in Figure 1a. In this preliminary study, we focus on the main lobes and areas, neglecting the interaction terms, corresponding to the off-diagonal blocks of the K-operator. Examining the results concerning the frontal lobe (1st block), we notice a decreased connectivity between the ventral anterior cingulate cortex and dorsal anterior cingulate cortex and between the last one and the frontal default model network. The role of the default mode network is key for healthy aging, including age effects for AD patients; its role has also been highlighted for timely diagnosis [24]. In the temporal lobe (2nd block) a connectivity decrease is visible between the left auditory region and the left default mode network. Lateralization of the default mode network is also linked to memory issues, as highlighted by joint cognitive and rest fMRI studies [2]. In the parietal lobe (3rd block) the most noticeable effects include a decreased connectivity between the right anterior intraparietal sulcus and the right parietal cortex. Particularly evident are the effects on the occipital lobe (4th block), with a decrease of connectivity between the striate and the right lateral occipital complex, and between the last one and the visual cortex. The occipital posterior also shows altered connectivity: increased with the striate and decreased with the other regions. Atrophy in the occipital cortex is present in AD patients, and the damage of its white matter is responsible for visual hallucinations [20]. The temporal lobe contains the hippocampus, whose role in AD was confirmed by the statistical analysis discussed in Section 2. Concerning subcortical and other (5th block) brain structures, the major effects concern the decreased connectivity between the right anterior insula and the right insula, and between the cerebellum and dorsal posterior cingulate cortex. In this part of the analysis, we included the insula inside the "subcortical and other structures." However, it is sometimes indicated as a lobe itself [17]. Computing the blocks with the row-by-column product (Figure 1c), we confirm a major damage on frontal default mode network, cingulate cortex, Broca's area, temporal sulcus, occipital lobe, auditory, insula, and cerebellum.

* We refer to the ROIs list in MSDL and Harvard-Oxford ('cort-maxprob-thr25-2mm') atlas to interpret our results about K blocks, see this Table.

For Patient B, the diagonal blocks of the K-operator present a decrease in connectivity between the superior frontal sulcus and the motor area (as for Patient A), between the last one and the right dorsolateral prefrontal cortex, and an increase in connectivity between the superior frontal sulcus and the Broca's area. In the temporal lobe, a slight connectivity diminution spread above the antidiagonal, mostly involving the auditory area and the left and right superior temporal sulcus. In the parietal lobe, we observe a connectivity diminution between the right parietal cortex and right anterior intraparietal sulcus and between the left and right intraparietal sulcus. Concerning the occipital lobe, both Patient A and B present, with different degrees, a connectivity diminution between the visual cortex and the right lateral occipital complex. Patient B presents a connectivity decrease between the occipital posterior and the striate. Finally, analyzing subcortical and other brain areas, we notice connectivity alterations (as randomization). The blocks computed with the row-by-column (Figure 1d) confirm a decreased connectivity involving right frontal pole, right dorsolateral prefrontal cortex, and occipital lobe.
Considering the Harvard-Oxford Atlas, and focusing on temporal, parahippocampal, and fusiform regions, the shape of the K-operator for case studies of Patient A and Patient B is shown in Figures and 2a and 2b. Patient Apresents a great decrease in connectivity between the inferior and the middle temporal gyrus. We also notice a decrease in connectivity between the posterior parahippocampal gyrus and the posterior (Patient A and B) and the temporal occipital fusiform cortex (Patient A). Both patients present an increase of connectivity between the temporal and the occipital part of the fusiform cortex, and an increase of connectivity, more evident for the B patient, between the temporal fusiform cortex posterior and the occipital fusiform gyrus, while the last one presents a diminished connectivity with respect to the temporal fusiform cortex posterior. Patient A presents a greatly diminished connectivity between the posterior parahippocampal gyrus and the temporal occipital fusiform cortex. A diminished connectivity concerning the parahippocampal gyrus has been investigated to compare mild cognitive impairment and AD patients concerning their role in memory loss [31]. Patient A and Patient B present a connectivity decrease between the temporal fusiform cortex anterior and the planum temporale. Discrepancies about increasing connectivity concerning the fusiform gyrus for MCI and AD patients have also been found [7].

Comparison and prediction. In [22], it was supposed a form of the K-operator for AD containing time-decay terms, to represent the progressive interruption of connection between neural agglomerates, following the death of neurons, and the interruption from their signal. Here, as expected, we observed a prevalence of connectivity diminution, accompanied by effects of randomization, also observed in the literature [11].
Machine learning approaches can help predict the precise shape of the operator, having functions on its elements. The learning step should based on N patients. Concerning the test step, given the connectivity matrix of a new patient at the baseline, the prediction of K can provide insights on the disease progression for that patient. Through these techniques, we can perform an "internal validation" of the K-operator, not only relying on medical literature but also on the similarity between predicted numerical entries of the operator and the actual evolution of the patient, comparing the predicted with the measured evolution of the disease.
As a simple example of the method, we test the prediction based on the K-operator and linear regression in a simple example. We give as input the connectivity matrix of a male patient 79 years old (Patient C), and, using our previous data, we predict his disease progression by approximating his K-operator. Then, we compare the estimated K with the effective one (Figure 3). In Figure 2d, the same comparison is performed in detail concerning the action of K on the parahippocampal, temporal, and fusiform areas of the brain. The agreement is satisfactory (Frobenius distance concerning the complete, not only block-diagonal K: 8.26 for the MSDL atlas. Focusing on the fusiform and parahippocampal regions (though the Oxford atlas), the predicted K restricted to these regions is presented in Figure 2(c) and (d), respectively. There are several similarities. Both predicted and measured matrices present a decrease of connectivity the temporal fusiform cortex posterior and the parahippocampal gyrus posterior. In AD literature, some discrepancies are found, with studies indicating a connectivity diminution between the considered areas [28] is verified, as well as the increase of connectivity concerning hippocampal and parahippocampal regions [9]. The parahippocampal area is related to semantic memory [19].
Finally, we compare K computed on four patients' temporal, parahippocampal, and fusiform areas to investigate some features related to the progression from CN to AD through MCI stages. From Figure 4, the progression from EMCI to LMCI involves hippocampal gyrus and temporal fusiform cortex as also highlighted in the statistical analysis; the passage from CN to EMCI is smoother (it is also confirmed by statistical results of statistics shown in Appendix). The more involved areas are the parahippocampal gyrus, the temporal fusiform cortex, and the inferior temporal gyrus. The last one is involved in MCI and during the prodromal stages of AD [27].

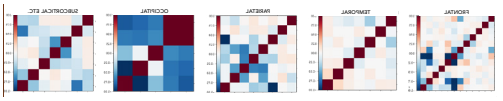

(a) Diagonal blocks of K for patient A, female, 63 years old.

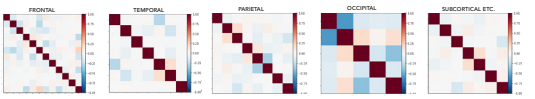

(b) Diagonal blocks of K for patient B, male, 73 years old.

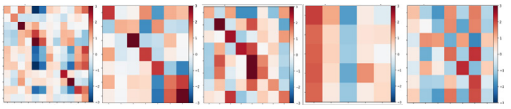

(c) K computed with the second product, patient A.

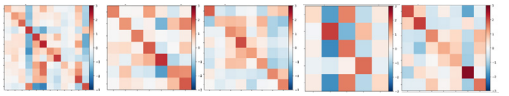

(d) K computed with the second product, patient B.

Fig. 1: K-operator acting on brain lobes and major regions (MSDL atlas), denoting the disease progression for Patients A (a) and B (b). Blocks computed with the row-by-column product, as a reference for clusters 'comparison, for Patients A (c) and B (d).

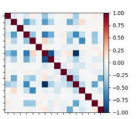

(a) Patient A, female, 63 years old

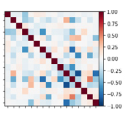

(b) Patient B, male, 73 years old.

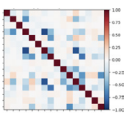

(c) Test patient, predicted

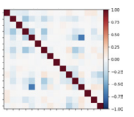

(d) Test patient, measured

Fig. 2: K-operator acting on temporal, parahippocampal, and fusiform regions (Harvard-Oxford atlas), for patient A (a) and B (b). On this information, given a test patient, a male of 79 years old (Patient C), the K-operator is predicted (c) and can be compared against the measured one (d).

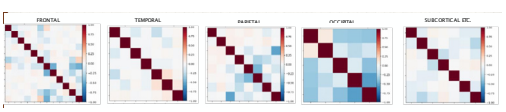

(a) Predicted

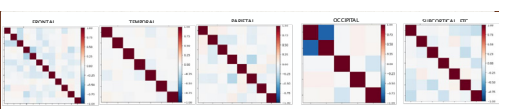

(b) Measured

Fig. 3: Diagonal blocks of the predicted (a) and measured (b) K-operator for a male patient of 79 years old (Patient C), MSDL atlas.

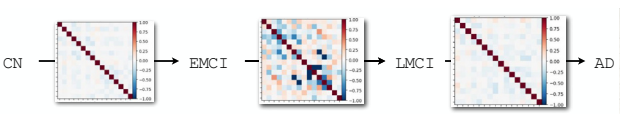

Fig. 4: Progression from CN to EMCI, LMCI, and Alzheimer-Perusini's disease for four different female patients (Patients D, E, F and G) in the same age range of 71-78 years old. The figures include temporal, parahippocampal, and fusiform areas according to the Harvard-Oxford atlas.

4. Discussion and Conclusions

Memory loss is a dramatic reality for patients affected by particular neurological diseases. In our research, we focused on Alzheimer's disease (called here Alzheimer-Perusini for historic reasons [3, 21]), obtaining information from functional magnetic resonance imagining and statistics, differentiating between mild cognitive impairment and disease progress, for patients of the ADNI dataset. We adopted a physics-inspired mathematical operator, K, recently proposed to model a generic neurological disease [22]; after some pioneering insights, we are applying it to the real dataset of ADNI. Our application confirms the findings of the medical literature, especially concerning the role of default mode network, posterior cingulate, and hypothalamus, both concerning healthy ageing and its disruption in AD [24], jointly with an effect of the disease on the temporal lobe and subcortical structures [28]. Results are also in line with statistical analysis performed on different classes of AD patients. From the comparison of our case studies, we noticed a decrease of connectivity involving superior frontal sulcus, dorsal anterior cingulate cortex, and between the dorsal and the ventral cingulate cortex. We also found a significant connectivity diminution between the visual cortex and the right lateral occipital complex, and between the occipital posterior and the striate, as well as a randomization of connectivity in subcortical and other brain areas. As a strategy for internal validation, we can define a prediction system using the K-operator as a prediction element for the disease progress. To provide a preliminary application of the idea, we proposed a linear regression based on the two considered cases, to approximate the K-operator for the connectivity matrix of a new patient. The computation of K can provide insights about the general form of neurological disease in mathematical terms. The search for a general, physics- inspired

approach toward neurological disease as brain network disruption could answer the wish for a more general approach in the literature [29]. Interdisciplinary approaches, such as statistical analysis and matrix-operator algebra, can help shed light on the complexity of neurological disease and, ultimately, on the fascinating complex of the human brain and mind. Future advancement of this strategy will involve a machine-learning application with a higher number of patients for the training set and its formalization of a multi-layer network [22].

Acknowledgements This paper was developed within the project funded by Next Generation EU – "Age-It – Ageing well in an ageing society" project (PE0000015), National Recovery and Resilience Plan (NRRP) – PE8 – Mission 4, C2, Intervention 1.3. The views and opinions expressed are only those of the authors and do not necessarily reflect those of the European Union or the European Commission. Neither the European Union nor the European Commission can be held responsible for them.

Data availability Data used for preparation of this article were obtained from the Alzheimer's Disease Neuroimaging Initiative (ADNI) database (https://adni.loni.usc.edu). As such, the investigators within the ADNI contributed to the design and implementation of ADNI and/or provided data but did not participate in the analysis or writing of this report. A complete listing of ADNI investigators can be found at: https://adni.loni.usc.edu/wp-content/uploads/how_to_apply/ ADNI_Acknowledgement_List.pdf.

Code availability The codes can be retrieved from GitHub.

Appendix A Tables contain statistical results discussed in Section 2.

Variables	NC (N = 186, 33.7%)	EMCI (N = 138, 25%)	LMCI (N = 125, 22.7%)	AD (N = 102, 18.5%)	p-value
Age (years)					
mean ± SD	73.5 ± 6.3	70.9 ± 6.8	71.3 ± 7.3	73.6 ± 8.2	2.3E-03†
[min, max]	[56, 89]	[56,89]	[55, 85]	[56, 90]	
Sex					
Male (%)	90 (48.4%)	78 (56.5%)	66 (52.8%)	57 (55.9%)	$4.8E-01$‡
Female (%)	96 (51.6%)	60 (43.5%)	59 (47.2%)	45 (44.1%)	
Education					
mean ± SD	16.6 ± 2.5	16.2 ± 2.6	16.5 ± 2.7	15.9 ± 2.6	$2.9E-01$†
[min, max]	[12, 20]	[11, 20]	[9, 20]	[9, 20]	
MMSE					
mean ± SD	29.0 ± 1.3	28.4 ± 1.6	27.6 ± 1.8	23 ± 2.1	≈ 0†
[min, max]	[24, 30]	[24, 30]	[24, 30]	[19, 26]	
Memory					
None	186 (100%)	1 (0.7%)	1 (0.8%)	0 (0%)	≈ 0‡
Questionable	0 (0%)	129 (93.5%)	98 (78.4%)	8 (7.8%)	
Mild-Moderate	0 (0%)	8 (5.8%)	26 (20.8%)	94 (92.2%)	
Orientation					
None	186 (100%)	87 (63%)	61 (48.8%)	6 (5.9%)	≈ 0‡
Questionable	0 (0%)	48 (34.8%)	53 (42.4%)	26 (25.5%)	
Mild	0 (0%)	3 (2.2%)	11 (8.8%)	70 (68.6%)	
Judgment&Problem Solving					
None	179 (96.2%)	58 (42%)	34 (27.2%)	0 (0%)	≈ 0‡
Questionable	7 (3.8%)	76 (55%)	86 (68.8%)	32 (31.4%)	
Mild	0 (0%)	4 (2.8%)	4 (3%)	70 (68.6%)	
Community& Affair					
None	183 (98.4%)	109 (79%)	73 (58.4%)	11 (10.8%)	≈ 0‡
Questionable	2 (1.1%)	28 (20.3%)	50 (40.0%)	43 (42.2%)	
Mild - Moderate	1 (0.5%)	1 (0.7%)	2 (1.6%)	48 (47%)	
Home&Hobbies					
None	185 (99.5%)	90 (65.2%)	68 (54.4%)	14 (13.7%)	≈ 0‡
Questionable	1 (0.5%)	43 (31.2%)	51 (40.8%)	28 (27.5%)	
Mild - Moderate	0 (0%)	5 (3.6%)	6 (4.8%)	60 (58.8%)	
Personal Care					
None	186 (100%)	137 (99.3%)	119 (95.2%)	78(76.5%)	$1.8E-15$‡
Mild - Moderate	0 (0%)	0(0%)	0 (0%)	0 (0%)	
Moderate	0 (0%)	1 (0.7%)	6 (4.8%)	24 (23.5%)	
CDR-SB					
mean ± SD	0.03 ± 0.13	1.33 ± 0.83	1.8 ± 1	4.5 ± 1.6	≈ 0†
[min, max]	[0, 1]	[0.5, 4]	[0.5, 4]	[1.5, 10]	

Table 1: Demographics and clinical characteristics of participants at baseline. * One-way ANOVA, † Kruskal-Wallis H test, ‡CHI-Square test

Variables	NC (N = 186, 33.7%)	EMCI (N = 138, 25%)	LMCI (N = 125, 22.7%)	AD (N = 102, 18.5%)	p-value
Ventricles					
mean (SD)	3.3E+04 (1.8E+04)	2.9E+05 (5.7E+04)	3.9E+04 (2.2E+04)	4.8E+04 (2.1E+04)	$2.3E-08$†
[min, max]	[7.8E+03, 1.1E+05]	[2.4E+05, 8.5E+05]	[9.2E+03, 1..0E+05]	[1.4E+04, 1.3E+05]	
Hippocampus					
mean (SD)	7.5E+03 (8.9E+02)	7.3E+03 (9.9E+02)	6.7E+03 (1.1E+03)	6.0E+03 (9.3E+02)	≈ 0*
[min, max]	[5.2E+03, 9.8E+03]	[4.7E+03, 9.5E+03]	[4.2E+03, 9.8E+03]	[4.1E+03, 8.4E+03]	
WBV					
mean (SD)	1.05E+06 (1.0E+05)	1.1E+06 (9.8E+04)	1.0E+06 (1.0E+05)	1.6E+06 (1.2E+05)	$2.0E-03$*
[min, max]	[7.8E+05, 1.3E+06]	[8.6E+05, 1.3E+06]	[8.4E+05, 1.3E+06]	[7.5E+05, 1.3E+06]	
Entorhinal					
mean (SD)	3.8E+03 (6.0E+02)	3.8E+03 (6.7E+02)	3.4E+03 (7.0E+02)	2.9E+03 (6.6E+02)	≈ 0*
[min, max]	[2.2E+03, 5.6E+03]	[2.0E+03,5.9E+03]	[1.5E+03, 5.4E+03]	[1.4E+03, 4.4E+03]	
Fusiform					
mean (SD)	1.9E+04 (2.3E+03)	1.9E+04 (2.7E+03)	1.8E+04 (2.8E+03)	1.6E+04 (2.4E+03)	$2.0E-10$*
[min, max]	[1.2E+04, 2.7E+04]	[1.2E+04, 2.7E+04]	[1.0E+04, 3.0E+04]	[1.0E+04, 2.2E+04]	
MidTemp					
mean (SD)	2.1E+04 (2.4E+03)	2.1E+04 (2.6E+03)	2.0E+04 (2.6E+03)	1.8E+04 (2.9E+03)	$3.3E-14$*
[min, max]	[1.6E+04, 2.9E+04]	[1.2E+04, 2.9E+04]	[1.0E+04, 3.0E+04]	[1.1E+04, 2.5E+04]	
ICV					
mean (SD)	1.5E+06 (1.6E+05)	1.5E+06 (1.5E+05)	1.5E+06 (1.6E+05)	1.5E+06 (1.7E+05)	$3.4E-01$‡
[min, max]	[1.2E+06, 1.9E+06]	[1.2E+06, 1.9E+06]	[1.2E+06, 2.1E+06]	[1.1E+06, 1.9E+06]	

Table 2: Baseline brain characteristics of participants. * One-way ANOVA, † Kruskal-Wallis H test, ‡CHI-Square test

References

[1] Badhwar, A., Tam, A., Dansereau, C., Orban, P., Hoffstaedtre, F., Bellec, P., 2017. Resting-state network dysfunction in Alzheimer's disease:A systematic review and meta-analysis. Alzheimer & Dementia 8, 73—85.

[2] Banks, S.J., Zhuang, X., Bayram, E., Bird, C., Cordes, D., Caldwell, J.Z.K., Cummings, J.L., Initiative, A.D.N., 2018. Default Mode Network Lateralization and Memory in Healthy Aging and Alzheimer's Disease. Alzheimer's Disease Neuroimaging Initiative 66, 1223–1234.

[3] Barone, P., et al., 2021. Neurologia Clinica. Idelson - Gnocchi, Naples.

[4] Berron, D., van Westen, D., Ossenkoppele, R., Strandberg, O., Hansson, O., 2020. Medial temporal lobe connectivity and its associations with cognition in early alzheimer's disease. Brain 143, 1233–1248.

[5] Bi, X.a., Xu, Q., Luo, X., Sun, Q., Wang, Z., 2018. Analysis of progression toward alzheimer's disease based on evolutionary weighted random support vector machine cluster. Frontiers in Neuroscience 12.

[6] Burke, S.N., Barnes, C.A., 2006. Neural plasticity in the ageing brain. Nature reviews neuroscience 7, 30–40.

[7] Cai, S., Chong, T., Zhang, Y., Li, J., von Deneen, K.M., Ren, J., Dong, M., Huang, L., 2015. Alzheimer's Disease Neuroimaging Initiative.Altered Functional Connectivity of Fusiform Gyrus in Subjects with Amnestic Mild Cognitive Impairment: A Resting-State fMRI Study. Frontiers in Human Neuroscience 9.

[8] Castellani, R.J., Rolston, R.K., Smith, M.A., 2010. Alzheimer disease. Disease-a-month: DM 56, 484.

[9] Dautricourt, S., de Flores, R., Landeau, B., Poisnel, G., Vanhoutte, M., Delcroix, N., Eustache, F., Vivien, D.,

de la Sayette, V., Ch´etelat, G.,
2021. Longitudinal Changes in Hippocampal Network Connectivity in Alzheimer's Disease. Annals of Neurology 90, 391–406.
[10] Echegoyen, I., L´opez-Sanz, D., Buld´u, J.M., 2021. From single layer to multilayer networks in mild cognitive impairment and Alzheimer's disease. Journal of Physics: Complexity 2, 045020.
[11] Fathian, A., Jamali, Y., Raoufy, M., et al., 2022. The trend of disruption in the functional brain network topology of Alzheimer's disease. Scientific Reports 12, 14998.
[12] van den Heuvel, M.P., Sporns, O., 2013. Network Hubs in the Human Brain. Trends in Cognitive Sciences 12, 683–696.
[13] Hojjati, S.H., Ebrahimzadeh, A., Khazaee, A., Babajani-Feremi, A., Initiative, A.D.N., et al., 2018. Predicting conversion from mci to ad by integrating rs-fmri and structural mri. Computers in biology and medicine 102, 30–39.
[14] Igarashi, K.M., 2023. Entorhinal cortex dysfunction in alzheimer's disease. Trends in neurosciences 46, 124–136.
[15] Jonker, C., Geerlings, M.I., Schmand, B., 2000. Are memory complaints predictive for dementia? a review of clinical and population-based studies. International journal of geriatric psychiatry 15, 983–991.
[16] Kennedy, D., Haselgrove, C., Breeze, J., Frazier, J., Seidman, L., Goldstein, J., . HarvardOxford cort maxprob thr25 2mm . URL: https: //fsl.fmrib.ox.ac.uk/fsl/fslwiki/Atlases.
[17] Kiernan, J.A., Rajakumar, N., 2015. Barr: Il Sistema Nervoso dell'Uomo. EdiSes.
[18] Lee, P., Ryoo, H., Park, J., Jeong, Y., Initiative, A.D.N., et al., 2017. Morphological and microstructural changes of the hippocampus in early mci: a study utilizing the alzheimer's disease neuroimaging initiative database. Journal of Clinical Neurology (Seoul, Korea) 13, 144.
[19] Li, M., Lu, S., Zhong, N., 2016. The Parahippocampal Cortex Mediates Contextual Associative Memory: Evidence from an fMRI Study. Biomed Research International 2016, 9860604.
[20] Lin, S.H., Yu, C.Y., Pai, M.C., 2006. The occipital white matter lesions in Alzheimer's disease patients with visual hallucinations. Clinical Imaging 30, 388–393.
[21] Lucci, B., 1998. The contribution of Gaetano Perusini to the definition of Alzheimer's disease. The Italian J. of Neurological Sciences , 49–52.
[22] Mannone, M., Fazio, P., Marwan, N., 2024. Modeling a Neurological Disorder as the Result of an Operator Acting on The Brain: A First Sketch Based on Network Channel Modeling. Chaos 35.
[23] Martin Prince, A., Wimo, A., Guerchet, M., Gemma-Claire Ali, M., Wu, Y., Prina, M., Yee Chan, K., Xia, Z., 2015. World alzheimer report 2015 the global impact of dementia an analysis of prevalence, incidence, cost and trends. Alzheimer's diease international .
[24] Mevel, K., Ch´etelat, G., Eustache, F., Desgranges, B., 2011. The default mode network in healthy aging and Alzheimer's disease. Int J Alzheimers Dis. 14.
[25] Phillips, M.L., 2012. Neuroimaging in psychiatry: bringing neuroscience into clinical practice. The British Journal of Psychiatry 201, 1–3.
[26] Rao, Y.L., Ganaraja, B., Murlimanju, B., Joy, T., Krishnamurthy, A., Agrawal, A., 2022. Hippocampus and its involvement in alzheimer's disease: a review. 3 Biotech 12, 55.
[27] Scheff, S., Price, D., Schmitt, F., Scheff, M., Mufson, E., 2011. Synaptic loss in the inferior temporal gyrus in mild cognitive impairment and Alzheimer's disease. J Alzheimers Dis. 24, 547–57.
[28] Schwab, S., Afyouni, S., Chen, Y., Han, Z., Guo, Q., Dierks, T., Wahlund, L.O., Grieder, M., 2020. Functional Connectivity Alterations of the Temporal Lobe and Hippocampus in Semantic Dementia and Alzheimer's Disease. J Alzheimers Dis. 76, 1461–1475.
[29] Seeley, W.W., 2017. Mapping Neurodegenerative Disease Onset and Progression. Cold Spring Harb Perspect. Biol. 9, 1–18.
[30] Varoquaux, G., Gramfort, A., Pedregosa, F., Michel, V., Thirion, B., 2011. Multisubject dictionary learning to segment an atlas of brain spontaneous activity. Information Processing in Medical Imaging , 562–573.
[31] Yang, H., Xu, H., Li, Q., Jin, Y., Jiang, W., Wang, J., Wu, Y., Li, W., Yang, C., Li, X., Xiao, S., Shi, F., Wang, T., 2019. Study of brain morphology change in Alzheimer's disease and amnestic mild cognitive impairment compared with normal controls. General Psychiatry 32, e100005.